

# Trajectory Tracking Control of a Quadrotor Using Feedback Linearization

R. Bonna<sup>1</sup> and J. F. Camino<sup>1</sup>

<sup>1</sup> School of Mechanical Engineering, University of Campinas - UNICAMP, 13083-860, Campinas, SP, Brazil.  
Email: ricardobonna@gmail.com, camino@fem.unicamp.br

*Abstract: This paper presents a nonlinear trajectory tracking control design for a quadrotor helicopter using feedback linearization. The quadrotor dynamics consists of two equations of motion, one for the translation and the other for the rotation. The dynamics for the rotational motion is fully actuated and decoupled from the equations for the translational motion. On the other hand, the translational dynamics is underactuated and depends on the rotational dynamics. In the first step of the control design, a feedback linearization law is used to linearize the rotational dynamics. Then, it is shown that an auxiliary control input that arises during that step can be used to linearize the translational dynamics through a second feedback linearization law. The small angle approximation is not required in this design. The proposed control law guarantees convergence of the quadrotor trajectory to a given reference trajectory. Numerical results show the benefits of the proposed control scheme.*

**Keywords:** quadrotor, unmanned aerial vehicle, underactuated system, nonlinear control, feedback linearization.

## INTRODUCTION

In recent decades, there has been an increasing interest in Unmanned Aerial Vehicles (UAV) due to its practical uses in various areas, ranging from military applications to traffic surveillance. A commonly used UAV is the quadrotor, which is a helicopter with four rotors. The quadrotor vehicle provides great maneuverability, since it allows vertical take off and landing. The rotors of the quadrotor are fixed on the ends of a cross-shaped frame, as shown in Figure 1.



Figure 1 – A commercial quadrotor.

In order to maneuver a quadrotor, a feedback control system is usually necessary. However, it is not an easy job to design a controller for this kind of vehicle. The dynamics is nonlinear and underactuated, leading to a system that is significantly more difficult to control than a fully actuated system. Underactuated systems are characterized by having more degrees of freedom than actuators (Fantoni and Lozano (2002)). This property generates interesting control problems that generally require nonlinear control design techniques.

For quadrotors, two major control problems emerge: attitude stabilization and trajectory tracking. Attitude stabilization consists in stabilizing the rotational dynamics of the quadrotor without taking into account the translational motion. For this class of problem, linear control techniques can be applied, such as PID control (Hua et al. (2013)) and LQ design methods (Bouabdallah et al. (2004)), as well as nonlinear control techniques, such as feedback linearization (Das et al. (2008)), quaternion based feedback control (Tayebi and McGilvray (2006)), nested saturation techniques (Castillo et al. (2005)), and sliding mode control (Zhang et al. (2011)).

Control techniques for trajectory tracking are usually more involved than those used for attitude stabilization. In fact, attitude stabilization controllers are normally used inside an inner control loop within a trajectory tracking control problem (Das et al. (2008), Mahony et al. (2012), Hua et al. (2013)). Trajectory tracking control problems can be handled using

nonlinear control techniques such as feedback linearization (Lee et al. (2009)), predictive and nonlinear robust control (Raffo et al. (2010)), adaptive control (Nicol et al. (2011)), backstepping techniques (Madani and Benallegue (2006a,b), Bouabdallah and Siegwart (2005)), and sliding mode control (Lee et al. (2009), Besnard et al. (2012), Bouabdallah and Siegwart (2005)).

The proposed trajectory tracking control design can be summarized as follows. A feedback linearization law is applied to the rotational dynamics, providing a second-order linear system with an auxiliary control input. Then, by differentiating twice the translational dynamics and using some components of the auxiliary control input, a second feedback linearization control law is applied to render the translational dynamics also linear. Using a typical trajectory tracking control law, the fourth-order tracking error dynamics, for the translational motion, is written in the state-space form. Finally, the control gains that guarantee convergence of the tracking error to zero are designed using the LQR technique.

It should be emphasized that the idea of differentiating twice the translational dynamics before applying a feedback linearization law has been used in Lee et al. (2009). However, unlike Lee et al. (2009), our approach does not require the small angle approximation, which is a major restriction for many applications.

## QUADROTOR DYNAMIC MODEL

Each of the four rotors of a quadrotor generates a thrust and a torque that are perpendicular to the quadrotor's body frame. The rotors, located at the opposite ends of the frame, spin in the same direction. Thus, two of them rotate clockwise and the other two counterclockwise. In this configuration, the rotors' thrusts are able to generate propulsion and three orthogonal torques.

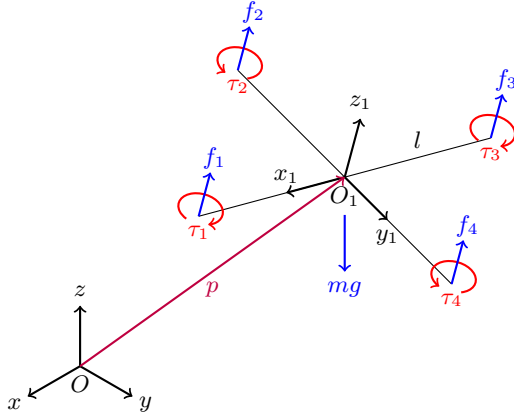


Figure 2 – Free body diagram showing the forces and torques generated by each rotor.

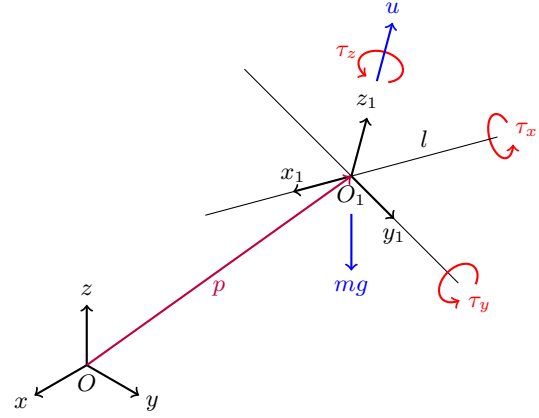


Figure 3 – Free body diagram showing the resulting forces and torques at the center of mass.

Two referential frames are used to derive the dynamics, one fixed to the body of the quadrotor, named  $O_1$ , and the other considered as inertial, named  $O$ . Figure 2 shows a schematic diagram containing the two reference frames,  $O$  and  $O_1$ , the forces  $f_i$  and the torques  $\tau_i$  generated by the rotors. The vector  $p = [p_x, p_y, p_z]^T$  is the position of the quadrotor's center of mass described in the inertial frame  $O$ . The torque  $\tau_i$ , proportional to the rotor's thrust  $f_i$ , is given by

$$\tau_i = c f_i$$

with  $c$  a force-to-torque scaling factor. By moving the forces  $f_i$  to the quadrotor's center of mass, as shown in Figure 3, the new control inputs  $u$ ,  $\tau_x$ ,  $\tau_y$  and  $\tau_z$  are given by the following invertible relation:

$$\begin{bmatrix} u \\ \tau_x \\ \tau_y \\ \tau_z \end{bmatrix} = \begin{bmatrix} 1 & 1 & 1 & 1 \\ 0 & -l & 0 & l \\ -l & 0 & l & 0 \\ -c & c & -c & c \end{bmatrix} \begin{bmatrix} f_1 \\ f_2 \\ f_3 \\ f_4 \end{bmatrix} \quad (1)$$

with  $l$  the distance between each rotor and the quadrotor's center of mass.

The nonsingular transformation matrix that changes the representation of a vector from the local frame  $O_1$  to the inertial frame  $O$  is given by

$$R(\alpha) = \begin{bmatrix} \cos \psi \cos \theta & -\sin \psi \cos \theta & \sin \theta \\ \sin \psi \cos \phi + \cos \psi \sin \theta \sin \phi & \cos \psi \cos \phi - \sin \psi \sin \theta \sin \phi & -\cos \theta \sin \phi \\ \sin \psi \sin \phi - \cos \psi \sin \theta \cos \phi & \sin \phi \cos \psi + \sin \psi \sin \theta \cos \phi & \cos \theta \cos \phi \end{bmatrix}$$

with  $\alpha = [\phi, \theta, \psi]^T$  the XYZ Euler-Cardan angles.

The angular velocity  $\omega$  of the reference frame  $O_1$  relative to the frame  $O$ , described in the local reference frame  $O_1$ , is given by

$$\omega = J(\alpha)\dot{\alpha} \quad (2)$$

with the Jacobian matrix given by

$$J(\alpha) = \begin{bmatrix} \cos \psi \cos \theta & \sin \psi & 0 \\ -\cos \theta \sin \psi & \cos \psi & 0 \\ \sin \theta & 0 & 1 \end{bmatrix}$$

Note that  $J(\alpha)$  is singular if  $\cos \theta = 0$ , which happens whenever the  $z_1$  axis is parallel to the  $x$  axis or, equivalently, orthogonal to the  $z$  axis.

The Euler equations, in the local reference frame  $O_1$ , is given by

$$I\dot{\omega} + \omega \times I\omega = \tau$$

with the quadrotor inertia matrix given by  $I = \text{diag}(I_{xx}, I_{yy}, I_{zz})$  and the control input given by  $\tau = [\tau_x, \tau_y, \tau_z]^T$ . These inputs are the external torques due to the rotors' thrusts. Substituting the angular velocity given by (2) into the Euler equations, the rotational dynamics becomes

$$IJ\ddot{\alpha} = (IJ\dot{\alpha}) \times (J\dot{\alpha}) - I\dot{J}\dot{\alpha} + \tau \quad (3)$$

Using Newton's second law of motion, in the inertial frame, and neglecting the gyroscopic effects due to the rotation of the rotors, the translational dynamics is given by

$$m\ddot{p} = mg\hat{k} + R\hat{k}u \quad (4)$$

with  $m$  the quadrotor's total mass,  $p$  the position vector of the quadrotor's center of mass,  $g$  the gravity acceleration,  $\hat{k} = [0, 0, 1]^T$  and  $u$  the total thrust.

It is important to emphasize that the rotational dynamics, given by (3), is fully decoupled from the translational dynamics, given by (4). However, the translational dynamics depends on the state  $\alpha$  of the rotational dynamics, through the transformation matrix  $R(\alpha)$ . The equation of motion of the quadrotor, given by (3) and (4), is used for control design in the next section. Notice that this is an underactuated system with six degrees of freedom and only four control inputs:  $u$ ,  $\tau_x$ ,  $\tau_y$ , and  $\tau_z$ .

## CONTROLLER DESIGN USING FEEDBACK LINEARIZATION

### Trajectory tracking control problem

The reference trajectory for the quadrotor is usually given as the desired position and orientation as a function of time. Since the quadrotor is a rigid body moving freely in the three-dimensional space, it has six degrees of freedom, three for translation and three for rotation. However, the quadrotor cannot follow any arbitrary trajectory, since it is an underactuated system that has only four control inputs. Nevertheless, it is possible to control four of its degrees of freedom. One common choice is to select the three components of the vector position  $p$  together with the yaw angle  $\psi$ . Therefore, our trajectory tracking control problem can be defined as follows: design the control inputs  $u$  and  $\tau$  so that the quadrotor position  $p$  and orientation  $\psi$  can asymptotically follow a given reference trajectory, defined by the vector  $p_r$  and the scalar  $\psi_r$ . This means that both  $p - p_r$  and  $\psi - \psi_r$  converge to zero with  $t \rightarrow \infty$ . It is assumed that the system states  $p$ ,  $\dot{p}$ ,  $\alpha$ , and  $\dot{\alpha}$  are all available for feedback.

### Feedback linearization technique

This section presents a control algorithm which is based on the feedback linearization technique, also called dynamic inversion. This technique (see Khalil (1996), Slotine and Li (1991)) consists in obtaining a nonlinear control law that makes the closed-loop system linear, so that linear control techniques can, afterward, be applied.

Consider the following second order nonlinear system

$$\ddot{x} = f(x, \dot{x}, t) + g(x, t)\eta \quad (5)$$

with  $x \in \mathbb{R}^n$ ,  $f : \mathbb{R}^{2n+1} \rightarrow \mathbb{R}^n$ ,  $g : \mathbb{R}^{n+1} \rightarrow \mathbb{R}^{n \times m}$  and  $\eta \in \mathbb{R}^m$ . If  $n = m$  and  $g(x, t)$  is invertible, then the control law

$$\eta = g(x, t)^{-1}(v - f(x, \dot{x}, t)) \quad (6)$$

transforms the nonlinear system (5) into the linear system

$$\ddot{x} = v$$

with  $v \in \mathbb{R}^n$  an auxiliary control input. Notice that, for an underactuated system, characterized by having less control inputs than degrees of freedom ( $m < n$ ), full feedback linearization cannot be applied. However, as in the case of a quadrotor, part of the dynamics can be linearized through feedback linearization.

## Control design

For the quadrotor, the rotational dynamics can be linearized through feedback linearization. Observe that (3) has the same form as (5) with

$$x = \alpha, \quad f(x, \dot{x}, t) = (IJ)^{-1}((IJ\dot{\alpha}) \times (J\dot{\alpha}) - I\dot{J}\dot{\alpha}), \quad g(x, t) = (IJ)^{-1}, \quad \eta = \tau$$

Thus, using (6), the control law is readily obtained as

$$\tau = IJv - (IJ\dot{\alpha}) \times (J\dot{\alpha}) + I\dot{J}\dot{\alpha} \quad (7)$$

with  $v = [v_\phi, v_\theta, v_\psi]^T$  an auxiliary control input. Substituting (7) into (3), gives

$$\ddot{\alpha} = v \quad (8)$$

with  $\alpha = [\phi, \theta, \psi]^T$ . Since our control problem requires that the tracking error  $e_\psi = \psi - \psi_r$  converges to zero for a given reference trajectory  $\psi_r$ , a suitable trajectory tracking control law  $v_\psi$  for

$$\ddot{\psi} = v_\psi$$

is given by

$$v_\psi = \ddot{\psi}_r - k_{\psi 2}(\dot{\psi} - \dot{\psi}_r) - k_{\psi 1}(\psi - \psi_r)$$

with  $k_{\psi 1}$  and  $k_{\psi 2}$  the control gains. Thus, the dynamics of the closed-loop tracking error  $e_\psi$  becomes

$$\ddot{e}_\psi + k_{\psi 2}\dot{e}_\psi + k_{\psi 1}e_\psi = 0 \quad (9)$$

Note that this is a second-order linear system whose sufficient and necessary conditions for stability are  $k_{\psi 1} > 0$  and  $k_{\psi 2} > 0$ . Since the vector  $v$  has three components, the same idea could have been applied to the other angles. However, in this paper, the extra two control inputs  $v_\phi$  and  $v_\theta$  are used together with  $u$  to enforce that the tracking error for the translational motion converges to zero.

For the translational dynamics, given by (4), the only available control input is  $u$ . However, by differentiating (4) twice, the control input  $v$  appears as follows:

$$\begin{aligned} mp^{(3)} &= H\dot{\alpha}u + R\hat{k}\dot{u} \\ mp^{(4)} &= \dot{H}\dot{\alpha}u + 2H\dot{\alpha}\dot{u} + H\ddot{\alpha}u + R\hat{k}\ddot{u} \end{aligned}$$

with  $p^{(n)}$  the time derivative of order  $n$  and the matrix  $H(\alpha)$  given by

$$H(\alpha) = \frac{\partial(R\hat{k})}{\partial\alpha} = \begin{bmatrix} 0 & \cos\theta & 0 \\ -\cos\theta\cos\phi & \sin\theta\sin\phi & 0 \\ -\cos\theta\sin\phi & -\sin\theta\cos\phi & 0 \end{bmatrix}$$

Denoting  $\ddot{u}$  by  $v_u$ , with  $v_u$  an auxiliary control input, and recalling that  $\ddot{\alpha} = v$ , we have

$$mp^{(4)} = \dot{H}\dot{\alpha}u + 2H\dot{\alpha}\dot{u} + Hvu + R\hat{k}v_u \quad (10)$$

Notice that the system states  $\psi$  and  $\dot{\psi}$  and the control input  $v_\psi$  do not appear in (10), since the last column of  $H$  is zero. Note also that the term  $Hvu + R\hat{k}v_u$  can be written as  $N\gamma$  with  $\gamma = [v_\phi, v_\theta, v_u]^T$  and  $N = [uH_{(1)}, uH_{(2)}, R\hat{k}]$  where  $H_{(i)}$  denotes the  $i$ -th column of matrix  $H$ . It should be emphasized that  $N$  is nonsingular whenever  $u \neq 0$  and  $\cos\theta \neq 0$ . Thus, (10) becomes

$$mp^{(4)} = \dot{H}\dot{\alpha}u + 2H\dot{\alpha}\dot{u} + N\gamma \quad (11)$$

which can be readily linearized using the control law  $\gamma$  given by

$$\gamma = N^{-1}(mV - \dot{H}\dot{\alpha}u - 2H\dot{\alpha}\dot{u}) \quad (12)$$

with  $V = [V_x, V_y, V_z]^T$  an auxiliary control input. Substituting (12) into (11) gives

$$p^{(4)} = V \quad (13)$$

Now, the control law  $V$  for the fourth-order linear system (13) can be appropriately designed. Since our control problem also requires that the tracking error  $e_p = p - p_r$  converges to zero for a given reference trajectory  $p_r$ , the trajectory tracking control law  $V$  is given by

$$V = p_d^{(4)} - K_4e_p^{(3)} - K_3\ddot{e}_p - K_2\dot{e}_p - K_1e_p \quad (14)$$

with  $K_i \in \mathbb{R}^{3 \times 3}$  the control gains. Thus, the dynamics of the closed-loop tracking error  $e_p$  is given by

$$e_p^{(4)} + K_4 e_p^{(3)} + K_3 \ddot{e}_p + K_2 \dot{e}_p + K_1 e_p = 0 \quad (15)$$

This dynamics can be represented in the following state-space form

$$\dot{e} = Ae + Bq, \quad q = -Ke \quad (16)$$

with

$$e = \begin{bmatrix} e_1 \\ e_2 \\ e_3 \\ e_4 \end{bmatrix}, \quad A = \begin{bmatrix} 0_3 & 1_3 & 0_3 & 0_3 \\ 0_3 & 0_3 & 1_3 & 0_3 \\ 0_3 & 0_3 & 0_3 & 1_3 \\ 0_3 & 0_3 & 0_3 & 0_3 \end{bmatrix}, \quad B = \begin{bmatrix} 0_3 \\ 0_3 \\ 0_3 \\ 1_3 \end{bmatrix}, \quad K = [K_1 \quad K_2 \quad K_3 \quad K_4]$$

the state vector defined as  $e_1 = e_p$ ,  $e_2 = \dot{e}_p$ ,  $e_3 = \ddot{e}_p$  and  $e_4 = e_p^{(3)}$ , the identity matrix of size  $n \times n$  denoted by  $1_n$ , and the zero matrix of size  $n \times n$  denoted by  $0_n$ .

As easily verified, system (16) is completely controllable. Thus, the gain  $K$  can be designed using any linear control design technique, such as the LQR design, which minimizes the cost function

$$J = \frac{1}{2} \int_0^\infty (e^T Q e + q^T R q) dt, \quad Q \geq 0, \quad R > 0$$

## NUMERICAL RESULTS

This section presents the stability and performance of the closed-loop system using two different reference trajectories and controller gains.

### System parameters

Table 1 shows the system parameters (borrowed from Madani and Benallegue (2006a)) used in the numerical simulations.

Table 1 – System parameters.

Parameter	Value	Units
$m$	2	$kg$
$I_{xx}$	1.2416	$kg.m^2$
$I_{yy}$	1.2416	$kg.m^2$
$I_{zz}$	2.4832	$kg.m^2$
$g$	9.81	$kg.m/s^2$
$c$	0.01	$m$
$l$	0.20	$m$

### Controller gains

To compute the gains  $k_{\psi 1}$  and  $k_{\psi 2}$ , the time-invariant second-order linear system (9) is first written in the following standard form

$$\ddot{e}_\psi + 2\xi\omega_n \dot{e}_\psi + \omega_n^2 e_\psi = 0$$

with  $2\xi\omega_n = k_{\psi 2}$  and  $\omega_n^2 = k_{\psi 1}$ . Now, by considering a damping factor  $\xi = 1$ , which avoid overshoots, and a natural frequency  $\omega_n = 3$ , which provides a reasonable settling time for a constant reference trajectory, the control gains are given by  $k_{\psi 1} = 9$  and  $k_{\psi 2} = 6$ .

The constant gains  $K_1$ ,  $K_2$ ,  $K_3$ , and  $K_4$  are computed using the LQR design. Note that the system of equations (15) can be decoupled if the gains  $K_i$  are diagonals, which occurs whenever the weighting matrices  $Q$  and  $R$  are both diagonals. After some preliminary simulations, the matrices are chosen as

$$Q = \text{blkdiag}(1_3, 0_3, 0.5 \times 1_3, 0_3)$$

$$R = 0.001 \times 1_3$$

where  $\text{blkdiag}(\bullet)$  denotes a block diagonal matrix. Theses weighting matrices provide a good settling time with small overshoot for a constant reference trajectory. The controller gains, obtained using these weighting matrices, are denoted by CG1 in Table 2. For the second set of gains in Table 2, denoted by CG2,  $w_n = 0.5$  and  $R = 1 \times 1_3$ . The other two parameters  $\psi$  and  $Q$  remain the same. The controller gains CG2 impose a stronger penalty on the control input.

Table 2 – Controller gains used in the simulations.

Controller Gains	$k_{\psi 1}$	$k_{\psi 2}$	$K_1$	$K_2$	$K_3$	$K_4$
CG1	9	6	$31.6228 \times 1_3$	$47.0352 \times 1_3$	$34.9796 \times 1_3$	$8.3642 \times 1_3$
CG2	0.25	1	$1.0001 \times 1_3$	$2.6762 \times 1_3$	$3.5811 \times 1_3$	$2.6762 \times 1_3$

## Reference trajectory

Two numerical simulations are presented. The first simulation illustrates the behavior of the closed-loop system using the controller gains CG1 under a time-varying reference trajectory. The second simulation compares the behavior of the closed-loop systems obtained using the controller gains CG1 and CG2. The reference trajectory used in this simulation is constant.

### Simulation 1: Time-varying reference trajectory

In this first simulation, the initial conditions are given by  $p(0) = [0, -1, 0]^T$ ,  $\dot{p}(0) = [0, 0, 0]^T$ ,  $\alpha(0) = [0, 0, 0]^T$ ,  $\dot{\alpha}(0) = [0, 0, 0]^T$ . It is considered that the quadrotor starts at a hovering state, which means  $u(0) = mg$  and  $\tau(0) = [0, 0, 0]^T$ . This simulation uses the controller gains CG1 and the time-varying reference trajectory given by

$$\begin{aligned} p_{xr}(t) &= \cos(t) \\ p_{yr}(t) &= \sin(t) \\ p_{zr}(t) &= \sqrt{t + 0.1} \\ \psi_r(t) &= \frac{\sin(t + 0.1)}{t + 0.1} \end{aligned}$$

Figure 4 shows the time-varying reference trajectory (dashed red line) and the quadrotor's position and yaw angle (solid blue line). As shown in Figure 4, the quadrotor's position  $p = [p_x, p_y, p_z]^T$  and the yaw angle  $\psi$  converge towards the time-varying reference trajectory. Similar conclusions may be drawn from Figure 5, that shows a three-dimensional plot of the reference trajectory  $p_r = [p_{xr}, p_{yr}, p_{zr}]^T$  (in red) and the position of the quadrotor's center of mass  $p = [p_x, p_y, p_z]^T$  (in blue).

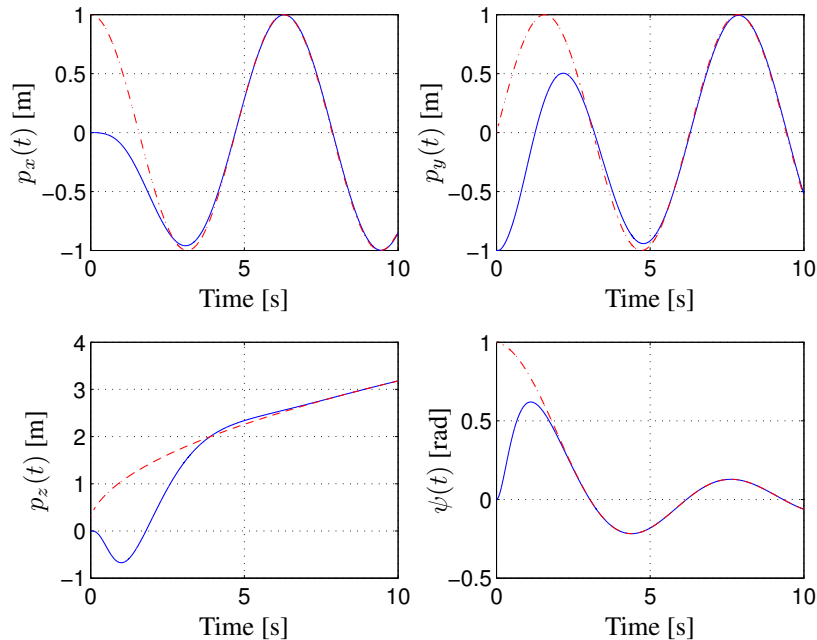


Figure 4 – Time-varying reference trajectory (dashed red line) and quadrotor's posture (solid blue line).

Figure 6 shows the rotors' thrusts for the time-varying reference trajectory. Note that, near  $t = 0$ , the magnitude of all the thrusts is larger than 100 N, but the magnitude of the steady-state values remains below 50 N. By changing the control gains  $k_{\psi 1}$ ,  $k_{\psi 2}$ ,  $K_1$ ,  $K_2$ ,  $K_3$ , and  $K_4$ , it is possible to decrease the magnitude of the control input. However, for this time-varying reference trajectory, the peaks seen in Figure 6, near  $t = 0$ , could not be avoided. Therefore, the influence of the controller gains on the control effort is investigated using a constant reference trajectory.

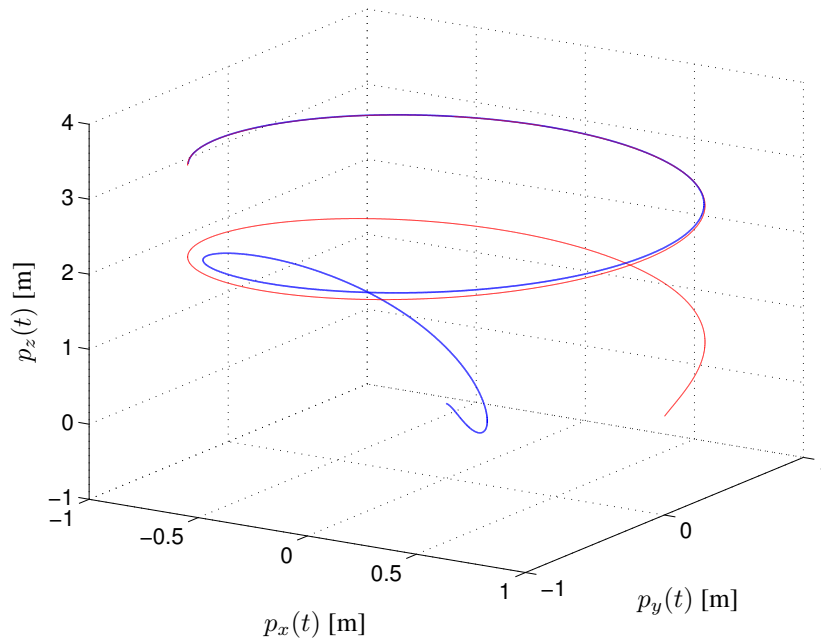


Figure 5 – Time-varying reference trajectory (in red) and quadrotor’s position (in blue).

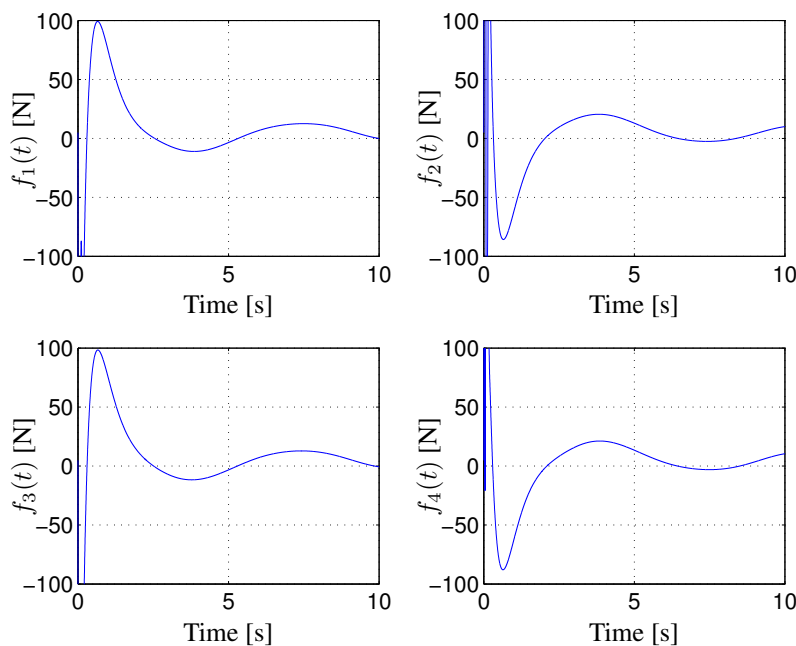


Figure 6 – Rotors’ thrusts for the time-varying reference trajectory.

### Simulation 2: Constant reference trajectory

This second simulation uses the two controller gains CG1 and CG2 given in Table 2. As previously explained, the controller gains CG2 imposes a stronger penalty on the control input. The initial conditions are zero. It is also considered that the quadrotor starts at a hovering state. The constant reference trajectory used in this simulation is given by  $[p_{xr}, p_{yr}, p_{zr}, \psi_r]^T = [5, 10, 15, 1]^T$ .

Figure 7 shows the constant reference trajectory (dashed red line), the quadrotor’s trajectory using the controller gains CG1 (solid blue line), and the quadrotor’s trajectory using the controller gains CG2 (dashed black line). In both cases, the quadrotor trajectory converged to the reference trajectory.

Figure 8 shows the rotors’ thrusts. The thrusts using the controller gains CG1 are represented by a solid line, and the thrusts using the controller gains CG2 by a dashed line. It can be seen that by changing the natural frequency  $\omega_n$  and the LQR weighting matrix  $R$ , which resulted in the controller gains CG2, the magnitude of the control input reduces, but the performance of the closed-loop system significantly deteriorates. Thus, the method gives the designer freedom to reduce the control input, if necessary, in detriment of closed-loop performance.

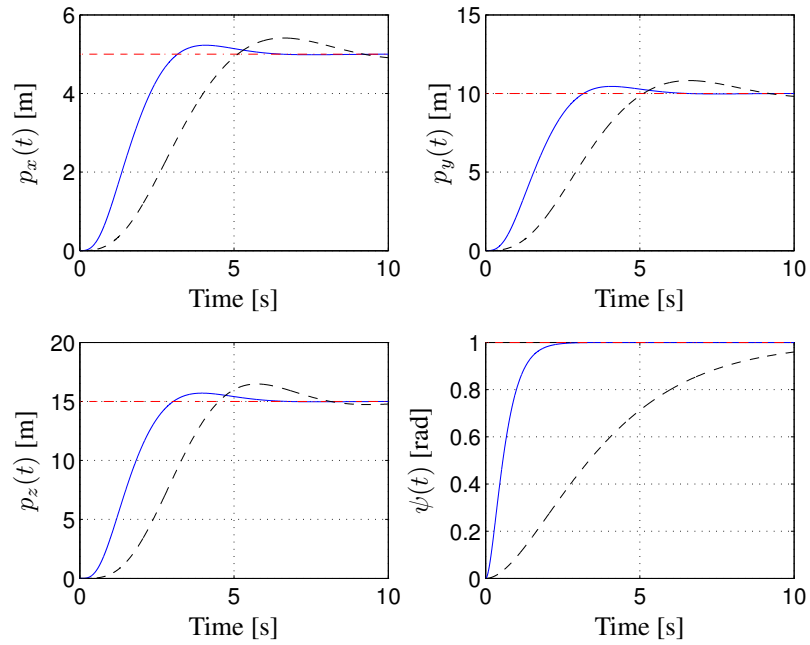


Figure 7 – Reference trajectory (dashed red line), quadrotor’s trajectory using CG1 (solid blue line) and using CG2 (dashed black line).

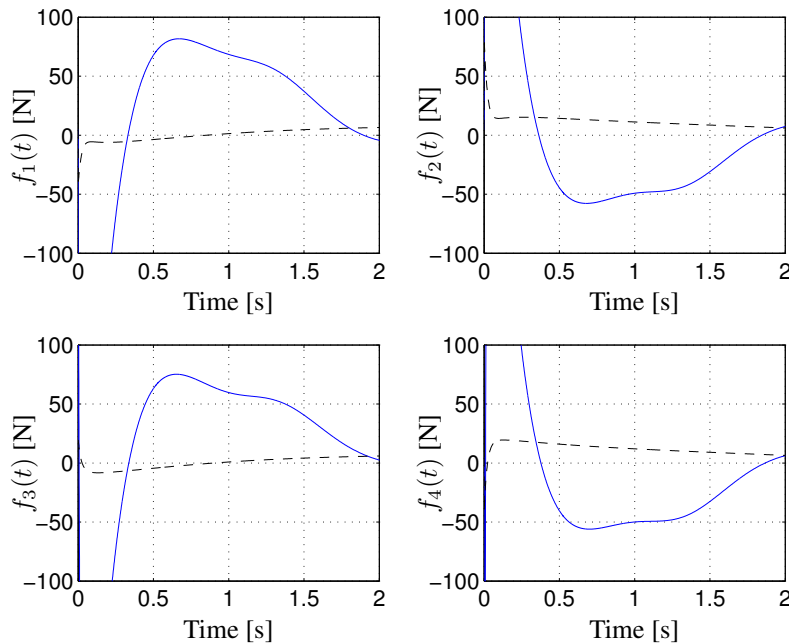


Figure 8 – Rotors’ thrusts for the constant reference trajectory using CG1 (solid blue line) and CG2 (dashed black line).

## CONCLUSION

This paper proposes a nonlinear control design, using feedback linearization, that guarantees convergence of the quadrotor trajectory to a given (sufficiently smooth) reference trajectory. The proposed design has the advantage that it does not assume the small angle approximation, commonly required in other techniques available in the literature. Even though the dynamics of the quadrotor is underactuated, meaning that the system has less control inputs than degrees of freedom, it is still possible to control four degrees of freedoms. In the proposed design, the quadrotor’s position and yaw angle are chosen as the reference trajectory. Through feedback linearization, the rotational and the translational dynamics are linearized. Using a typical trajectory tracking control law, the dynamics of the tracking error is derived. The LQR design is used to compute the control gains that stabilize the dynamics of the tracking error. Numerical simulations show that the method gives the designer some freedom to increase performance at the cost of control effort.

## RESPONSIBILITY NOTICE

The author(s) is (are) the only responsible for the printed material included in this paper.



## REFERENCES

- Besnard, L., Shtessel, Y. B. and Landrum, B. (2012). Quadrotor vehicle control via sliding mode controller driven by sliding mode disturbance observer, *Journal of The Franklin Institute* **349**(2): 658–684.
- Bouabdallah, S., Noth, A. and Siegwart, R. (2004). PID vs LQ control techniques applied to an indoor micro quadrotor, *IEEE/RSJ International Conference on Intelligent Robots and Systems*, Sendai, Japan, pp. 2451–2456.
- Bouabdallah, S. and Siegwart, R. (2005). Backstepping and sliding-mode techniques applied to an indoor micro quadrotor, *IEEE International Conference on Robotics and Automation*, Barcelona, Spain, pp. 2247–2252.
- Castillo, P., Lozano, R. and Dzul, A. (2005). *Modeling and Control of Mini-Flying Machines*, Springer-Verlag, London, UK.
- Das, A., Subbarao, K. and Lewis, F. (2008). Dynamic inversion with zero-dynamics stabilization for quadrotor control, *IET Control Theory and Applications* **3**(3): 303–314.
- Fantoni, I. and Lozano, R. (2002). *Non-linear Control for Underactuated Mechanical Systems*, Springer-Verlag, London, UK.
- Hua, M. D., Hamel, T., Morin, P. and Samson, C. (2013). Introduction to feedback control of underactuated VTOL vehicles, *IEEE Control Systems Magazine* **33**(1): 61–75.
- Khalil, H. K. (1996). *Nonlinear Systems*, Prentice-Hall, Upper Saddle River, NJ, USA.
- Lee, D., Kim, H. J. and Sastry, S. (2009). Feedback linearization vs. adaptive sliding mode control for a quadrotor helicopter, *International Journal of Control, Automation, and Systems* **7**(3): 419–428.
- Madani, T. and Benallegue, A. (2006a). Backstepping control for a quadrotor helicopter, *IEEE/RSJ International Conference on Intelligent Robots and Systems*, Beijing, China, pp. 3255–3260.
- Madani, T. and Benallegue, A. (2006b). Control of a quadrotor mini-helicopter via full state backstepping technique, *IEEE Conference on Decision and Control*, San Diego, CA, USA, pp. 1515–1520.
- Mahony, R., Kumar, V. and Corke, P. (2012). Multirotor aerial vehicles: Modeling, estimation, and control of quadrotor, *IEEE Robotics and Automation Magazine* **19**(3): 20–32.
- Nicol, C., Macnab, C. J. B. and Ramirez-Serrano, A. (2011). Robust adaptive control of a quadrotor helicopter, *Mechatronics* **21**(6): 927–938.
- Raffo, G. V., Ortega, M. G. and Rubio, F. R. (2010). An integral predictive/nonlinear  $H_\infty$  control structure for a quadrotor helicopter, *Automatica* **46**(1): 29–39.
- Slotine, J. J. and Li, W. (1991). *Applied Nonlinear Control*, Prentice-Hall, Englewood Cliffs, NJ, USA.
- Tayebi, A. and McGilvray, S. (2006). Attitude stabilization of a VTOL quadrotor aircraft, *IEEE Transactions on Control Systems Technology* **14**(3): 562–571.
- Zhang, R., Quan, Q. and Cai, K.-Y. (2011). Attitude control of a quadrotor aircraft subject to a class of time-varying disturbances, *IET Control Theory and Applications* **5**(9): 1140–1146.